AUT Journal of Mechanical Engineering

AUT J. Mech. Eng., 9(2) (2025) 195-210
DOI: 10.22060/ ajme.2025.23532.6143

Ultrasonic Vibratory Drilling Carbon Fiber/Graphene Nanoparticle Reinforced Polymers to Produce Desired Hole Quality: Experimental Analysis and Optimization

Mohammad Baraheni[1]*, Saeid Amini [2]

[1] Department of Manufacturing, Faculty of Mechanical Engineering, Arak University of Technology, Arak, Iran
[2] Department of Manufacturing, Faculty of Mechanical Engineering, University of Kashan, Kashan, Iran.

ABSTRACT: Carbon fiber-reinforced polymers are widely used in advanced applications due to their superb specifications. One of the principal problems in drilling such polymers is delamination which deteriorates the composite strength and can lead to part rejection during assembly. Ultrasonic vibration-assisted drilling is a newly developed machining method that induces higher workpiece quality. In this study, a comprehensive experimental examination was conducted with both mechanical and materialistic views. The materialistic parameters include graphene nanoparticles and lay-up arrangement. Furthermore, the mechanical parameters include drilling feed rate, tool type, and ultrasonic vibration. To follow this aim, different carbon fiber-reinforced polymer specimens were fabricated with various lay-up arrangements and graphene nanoparticle amounts. Besides, an analysis of variance was utilized to indicate the significant parameters. The results showed that the feed rate has the most effect on thrust force and delamination damage. Besides, graphene nanoparticles% and tool type were the significant parameters of delamination. To find the optimal settings, grey relational analysis was used. That was suggested to produce carbon fiber-reinforced polymer segments with symmetrical lay-up arrangements to reduce delamination damage. Furthermore, a lower feed rate value with 5% cobalt high-speed steel tool was suggested. Exerting ultrasonic vibration on the tool was also beneficial to improve the hole quality.

Review History:

Received: Sep. 22, 2024
Revised: Jan. 16, 2025
Accepted: Jan. 26, 2025
Available Online: Feb. 21, 2025

Keywords:

Delamination
Graphene Nanoparticle
Ultrasonic Drilling
Multi-Objective Optimization
Grey Relational Analysis

1- Introduction

Composites are considered key materials in different industry applications, especially in the aviation industry which is due to their high fatigue strength and also excellent strength-to-weight ratio [1]. Composites are in various types based on the used matrix which mostly include metal and polymer. Polymer-based composites offer different functionalities due to the combinations of fillers that widen their application. Fillers in composites are in fiber and particle types. In addition, fiber-reinforced composites have suitable potential for high-tech products in the power industry, automotive, aerospace, marine, and other sectors. [2].

The most prevalent fibers exercised in recent years include glass, carbon, nylon, Kevlar (aramid), polyester, and natural fibers. Lately, carbon fiber-reinforced polymers (CFRP) have been introduced to offer advanced applications. For instance, in the aviation industry, carbon fibers were used in aircraft wing boxes and vertical and horizontal stabilizers. About 22% of the airframe in Airbus A380 includes CFRP [3]. In CFRPs, up to 80 % of strength is related to carbon fibers. The used matrix in CFRP is as a bonding phase which keeps fibers next to each other. Moreover, the composite segment strength is in the fiber's direction which shows the importance of proper fiber orientation and layer lay-up [4]. In unidirectional situations, the stiffness and strength of CFRP are in one orientation [5]. However, in bi-directional situations, the fibers are in two perpendicular directions (90°), and the CFRP strength is high in two directions but not the same necessarily [6]. Hence, lay-up arrangement plays a main role in the strength of the CFRP component which also influences on machinability of the component. Nevertheless, the CFRP lay-up arrangement depends upon the component application which restricts the fiber's orientation. Besides, drilling operation parameters should be specified according to the desired condition.

Nanomaterials are newly developed materials that propose high-tech specifications for Fiber Reinforced Polymers (FRC). Different industries such as the aerospace and automotive industry have used nanomaterials in their applications. That was reported nanocomposites usage is growing from 225,060 metric tons (2014) to 585,984 metric tons (2019) [7]. In nanocomposites, at least one dimension of the nanoparticle is smaller than 100 nanometers. Nanoparticles improve different composite specifications including optical [8], mechanical [9], electrical [10], and thermal [11] properties. This improvement is because of the high surface-

*Corresponding author's email: mbaraheni@arakut.ac.ir

to-volume ratio [12]. This change in composite attributes by adding nanoparticles, leads to a change in drilling behavior which depends on the nanoparticle type and other composite conditions. Among nanoparticles, graphene is from the famous ones that is used in different applications such as electronics, mechanics, optical, and biomedical engineering. Graphene was determined as the latest member of the carbon family. Graphene compared to carbon nanotubes which are other allotrope of carbon structure, has more advantages that is because of larger surface area. That was also stated graphene nanoparticle is the stiffest material used in pressure barriers [13]. In addition, using graphene in nanocomposites is affordable.

In the assembly stage, a large number of holes are needed to be created for rivets and bolted joints which requires drilling operation. For instance, a passenger jet needs 1.5 to 3 million holes to be drilled [14]. The problems in FRC drilling arise from the hard nature of fibers and heterogeneous distribution in the matrix that induces damages such as delamination, fiber/matrix breakage, and fuzzing. Dimensional accuracy and surface quality of the holes in FRCs are influenced by drilling-induced damages especially delamination that leads up to 60% of all part rejection at assembly step [15]. Besides, tool wear mostly occurs in FRC machining which is related to the abrasive nature of FRCs [16]. Therefore, selecting proper tool material, tool geometry, and machining conditions is necessary for improving produced hole quality in FRCs. Other damages are also produced while drilling FRCs which include fuzzing, chipping, spalling, fiber-matrix debonding, etc. The mentioned damages lead to component performance reduction in the long term. In this regard, various machining methods have been proposed by researchers and industrials. Ultrasonic vibration-assisted drilling (UVAD), abrasive waterjet machining, high-speed drilling are the advanced methods in drilling FRCs in recent years [5, 17, 18]. UVAD process poses advantages such as machining force and torque reduction, chip removal performance improvement, drilling temperature reduction, tool life extension, and hole wall surface quality enhancement.

Numerous studies have been carried out on hole quality produced while drilling FRCs. Kavad et al. [19] conducted a review of process parameters' effect on drilling hole quality with different machining methods. Arul et al. [20] reported that feed rate increases cause thrust force increases in drilling polymeric composites. Mohan et al. [21] also studied machining parameters' effect on thrust force and delamination in drilling GFRP using the Taguchi method. That was found rotational speed and diameter of the drilling tool are the most significant parameters. Delamination analysis was also conducted by various researchers [22, 23]. Srinivasan et al. [24] examined delamination in propylene reinforced by glass fiber. Shetty et al. [25] also studied on delamination in CFRP which was conducted by two tool types including High-Speed Steel (HSS) and carbide tool. In this regard, Hocheng et al. [26] have published a comprehensive paper about different aspects of delamination in composites. Verma et al. [27] found an optimum machining condition for drilling GFRP by the fuzzy method. Moreover, in the research by Davim et al. [28], the machining parameters' effect on delamination in CFRP was investigated by using the Taguchi method and Analysis Of Variance (ANOVA). Dhawan et al. [29] examined delamination on two different composites by two lay-ups in different machining conditions and compared the results by the Artificial Neural Network (ANN) method. Mayuet et al. [30] also stated delamination at the entry and exit section of the drilled hole was improved at a lower feed rate and spindle speed. UVAD approach is preferred for CFRPs because of suitable machining performance. Cong et al. [31] investigated on rotary ultrasonic drilling of CFRP and compared with twist drill. Huang et al. [32] examined tool wear in UVAD of CFRP and compared with traditional drilling. That was observed tool flank wear was reduced about 13% comparing to traditional drilling.

According to the literature review of the previous works, that is indicated drilling CFRP requires comprehensive study considering materialistic and mechanical factors. In this investigation, both kinds of factors regarding GNP incorporation, lay-up arrangement, and machining factors in conventional drilling (CD) and UVAD processes will be evaluated experimentally and statistically. In addition, an attempt will be made to find out the optimal condition regarding the minimization of thrust force and delamination. In this regard, multi-objective optimization using grey relational analysis will be performed.

2- Materials and Methods

The produced samples contain ML 506-type epoxy resin with T700-type unidirectional carbon fibers and Graphene nanoplatelets (GNP). The CFRP plates were fabricated in-house using a hand lay-up technique followed by curing under controlled pressure and temperature. The GNPs were mixed with epoxy resin using high-shear mixing to ensure uniform dispersion before being impregnated into the carbon fiber layers. The samples are provided in plate geometry in dimensions of 200 × 200 and thickness of 2 millimeters. Besides, the samples are in $[0_2,90_2]$ stacking sequence. However, the stacking sequence for plates is divided into two arrangements including: symmetrical and asymmetrical. The specimens are in two types: CFRP and CFRP with 0.25% nanographene particles. The mentioned nanoparticle percentage was selected based on the previous researches [33] to prevent agglomeration. The graphene nanoparticles used in this study have a high purity of 98.5%, with a surface area of 40 m^2/g, a thickness of less than 60 nm, and a lateral size of 7 µm. The epoxy resin (ML506) has a density of 1.11 g/cm^3, a tensile strength of 75 MPa, a tensile modulus of 2.82 GPa, and a coefficient of thermal expansion of 12×10^{-6} 1/°C. The T700 carbon fibers feature a density of 1.8 g/cm^3, a tensile strength of 3800 MPa, a tensile modulus of 210 GPa, a coefficient of thermal expansion of 0.15×10^{-5}1/°C, and a thickness of 0.2 mm. The used drilling tools in this investigation are listed in Table 1. The experimental tests have been conducted on a FP4M CNC milling machine. Fig. 1 shows the experimental setup.

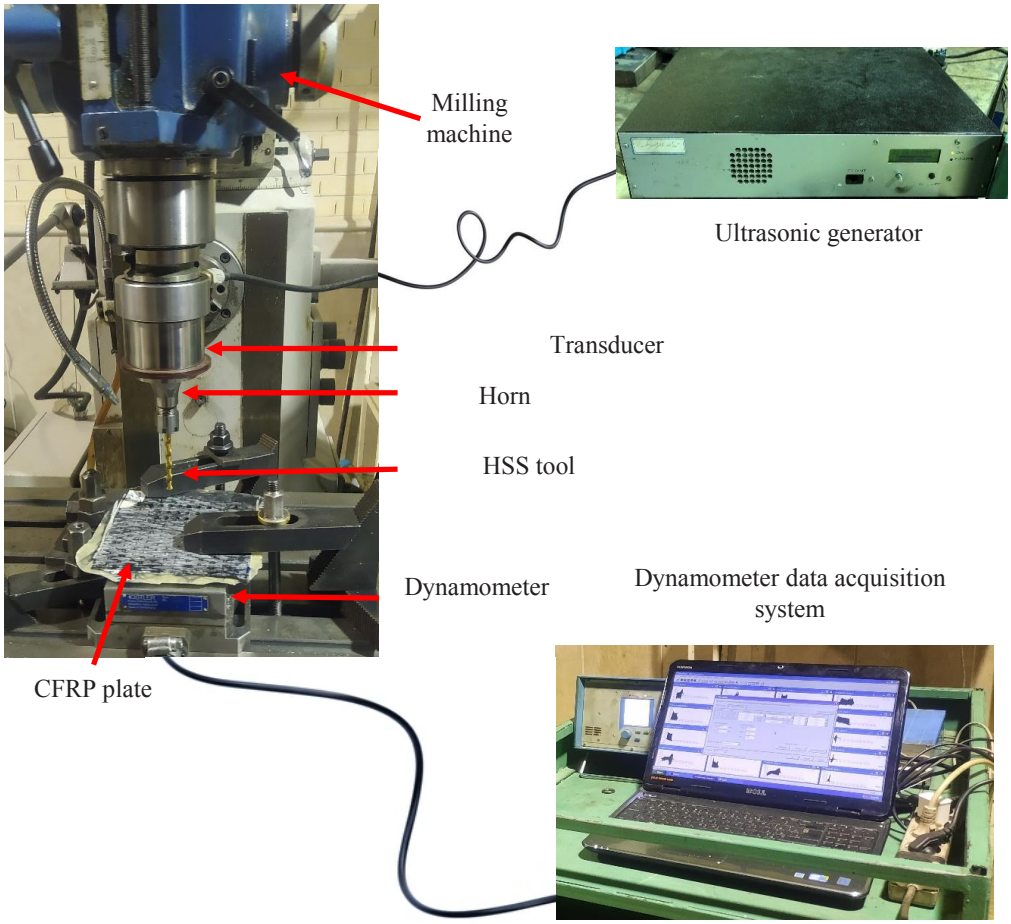

Fig. 1. Experimental setup

Table 1. Properties of the used tools.

Tool types	Diameter
HSS, HSS-5%Co, HSS-8%Co	6 mm

To apply ultrasonic vibration to the tool during rotation, a specially designed transducer was employed, which was connected to an ultrasonic vibration generator. The generator used was of the AMMM type, produced by MPI Company, with specifications suitable for high-frequency operations. To ensure efficient ultrasonic power transmission from the transducer to the drilling tool, an exponentially shaped horn was utilized. The horn's geometry was critical for amplifying the vibration amplitude while maintaining the desired frequency. To determine the optimal geometry for the horn, a modal analysis was conducted using ANSYS R17.0 software. The modal analysis accounted for the material properties of the horn, boundary conditions, and the operating frequency of the generator. The simulation identified a resonance frequency of 19816 Hz, and the corresponding mode shape showed longitudinal vibration along the tool axis. The largest deformation was observed at the horn's tip, confirming effective vibration transmission to the drilling tool. These results were crucial for ensuring that the ultrasonic vibrations were concentrated at the cutting interface, improving machining performance. The horn material was chosen as Al-7075, known for its high strength-to-weight ratio and excellent vibration transmission capabilities. After manufacturing the horn (weight = 168 gr), the experimental setup was fine-tuned to adjust the resonance frequency to 21 kHz, matching the operational requirements of the generator and transducer system. The tool's vibrating amplitude, measured using a gap sensor, was approximately 6 µm, confirming that the system effectively delivered high-frequency, low-amplitude vibrations to the cutting tool. To enhance the clarity of the experimental setup, we have included the vibration analysis

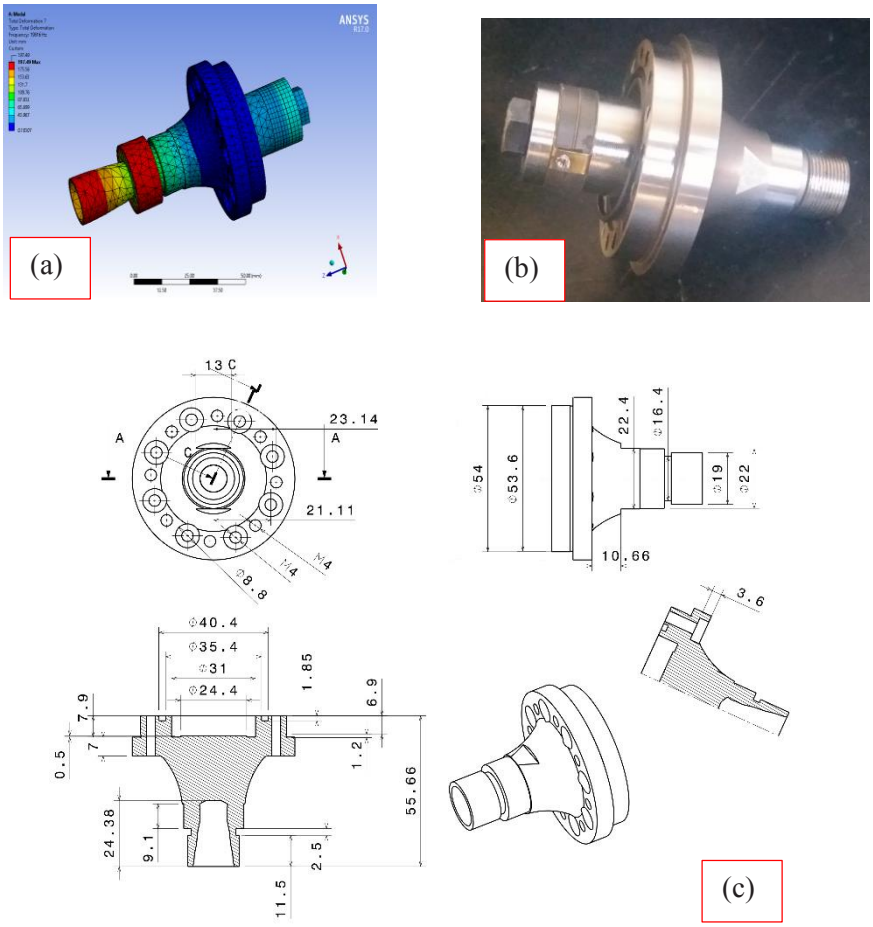

Fig. 2. a) the modeled horn in ANSYS Workbench software, b) fabricated horn, c) horn dimensions.

results for the horn, including the mode shape and frequency response, in the revised manuscript (see Fig. 2). This provides a complete picture of the transducer design, horn optimization, and vibration analysis, addressing the reviewer's concerns.

The process variables are divided into two groups including machining and composite variables (Table 2).

The parameters listed in Table 2 have been clarified in the following:

- **Feed Rate:** Three levels (0.08, 0.15, and 0.25 mm/rev) were chosen to evaluate the impact of material removal rate on thrust force and delamination.
- **Tool Type:** Three variations of HSS tools (standard HSS, 5% cobalt, and 8% cobalt) were used to assess the influence of tool material on cutting performance.
- **GNP Content:** Two levels (0% and 0.25%) were selected based on previous research to explore the effect of graphene reinforcement on the mechanical properties of CFRPs and its influence on machining performance.
- **Lay-up Arrangement:** Symmetric ($[0/90]_2$) and asymmetric ([0/90/0/90]) lay-ups were tested to study the effect of fiber orientation on thrust force and delamination.
- **Ultrasonic Vibration:** Two levels (on and off) were included to compare the performance of Ultrasonic vibration-assisted drilling and conventional drilling.

That should be noted the ultrasonic-assisted process is called Ultrasonic Vibration-Assisted Drilling (UVAD) and the other is called Conventional Drilling (CD). The experimental design is based on a full factorial mixed-level approach, which allows for the evaluation of the effects of multiple factors at various levels. Specifically, the parameters studied include feed rate, tool type, GNP content, lay-up arrangement, and ultrasonic vibration. Each combination of these parameters was tested, resulting in 72 experimental runs, as presented in Table 3. This design enables the investigation of both main effects and interaction effects on thrust force and delamination.

Eason 2D Visual Measurement Machine (VMM) was used to measure delamination value. The VMM was designed for magnification of 0.7x-4.5x. To assess delamination value, initially, several points around the damaged area were selected. Subsequently, Rasson 2D software is used to draw a circle by the least square method. Finally, the corresponding circle diameter is divided by the drill diameter. Therefore, the delamination value will be obtained which is called F_d [34].

Moreover, Scanning Electron Microscopy (SEM) is used to examine the nanoparticles and carbon fibers in the epoxy

Table 2. Process variables.

Variable	Level		
	1	2	3
Machining variables			
Ultrasonic vibration	Off	On	-
Tool type	HSS	HSS-5% Co	HSS-8% Co
Feed rate (mm/rev)	0.08	0.15	0.25
Composite variables			
GNP wt.%	0	0.25	-
Arrangement	Asymmetric	Symmetric	-

resin. The role of SEM analysis is to validate the quality and distribution of GNPs within the CFRP matrix. This ensures that the nanocomposite fabrication achieved a homogeneous dispersion of GNPs, which is critical for the study's mechanical and machining evaluations. Additionally, the SEM images provide evidence of fiber/matrix impregnation quality, supporting the study's focus on the influence of material properties on machining performance. One of the reasons that SEM is preferred to analyze particle size is because of its high resolution up to 10 nm.

In the present study, GRA method was employed to find an optimal condition. This method is used to convert the multi-objective problem into a single-objective one. GRA has been used in various areas such as agriculture, economy, engineering, etc.

To normalize the objective results, the corresponding "lower is better" condition, Eq. (1) will be used:

$$x_i(j)=\frac{y_i(j)-\min y_i(j)}{\max y_i(j)-\min y_i(j)}. \quad (1)$$

where $x_i(j)$ is the normalization value, min $y_i(j)$ is the lowest value of $y_i(k)$ for the jth result, and max $y_i(j)$ is the highest value of $y_i(j)$ for the jth result. In this study, i = 1, 2 (number of objectives) and j = 1, 2, 3, . . ., 72 (number of tests).

Subsequently, the grey relational coefficient (GRC) is calculated that demonstrates the relationship between the normalized value for one objective and the ideal value of the considered objective that is one. GRC is computed by Eq. (2):

$$\zeta_i(j)=\frac{\Delta_{min}-\lambda\Delta_{max}}{\Delta_{0i}(j)-\lambda\Delta_{max}} \quad (2)$$

$$\Delta_{0i}(j)=x_0(k)-x_i(k) \quad (3)$$

where λ is the weight factor ($0\le\lambda\le1$), Δ_{min} is the lowest value of Δ_{0i}, and Δ_{max} is the largest value of Δ_{0i}. In this study, that is assumed: $\lambda=0.5$

Afterwards, grey relational grade (GRG) is calculated by Eq. (4):

$$\gamma_i=\frac{1}{ni}\sum_{k=1}^{n}\zeta_i(j) \quad (4)$$

where n is number of the objectives. A higher GRG value indicates the closest factor to the optimal value.

3- Results and discussion

In this section, materialistic and machining parameters effects will be discussed separately. The resultant factors include thrust force and delamination. To discuss about each parameter effect, the main effects plot is used that simplifies demonstrating parameters influence. In other words, that is a plot of average result values at each level of a process variable. Besides, from the main effects plot, the relative strength of the effects of different parameters can be acquired.

3- 1- SEM images analysis

SEM images were captured and analyzed in order to identify the nanoparticles distribution in CFRP specimens. Fig. 3 shows SEM images from CFRP samples without nano-graphene particles. Fig. 3(a) shows a cross-section of CFRP laminates in magnification of 125x that comprises carbon fibers bonded with epoxy resin. Fibers on the top are not saturated aptly by epoxy resin which is due to the higher viscosity of the epoxy resin. That prevents epoxy adhesive penetration between carbon fibers and causes weak bonding. Consequently, while applying mechanical force, the fibers fail via the weak parts in the composite. However, the fibers

Table 3. Experimental design and correspondent results.

No.	Composite factors		Machining variables			Results		No.	Composite factors		Machining variables			Results	
	GNP%	Lay-up	Ultrasonic	Tool	Feed rate	Force	F_d		GNP%	Lay-up	Ultrasonic	Tool	Feed rate	Force	F_d
1	0	A*	1	8%	0.08	78	1.027	37	0.25	A	1	8%	0.08	99	1.033
2	0	A	1	8%	0.15	167	1.031	38	0.25	A	1	8%	0.15	125	1.071
3	0	A	1	8%	0.25	102	1.040	39	0.25	A	1	8%	0.25	168	1.064
4	0	A	0	8%	0.08	138	1.034	40	0.25	A	0	8%	0.08	97	1.033
5	0	A	0	8%	0.15	171	1.049	41	0.25	A	0	8%	0.15	114	1.039
6	0	A	0	8%	0.25	302	1.034	42	0.25	A	0	8%	0.25	155	1.050
7	0	A	1	5%	0.08	63	1.051	43	0.25	A	1	5%	0.08	148	1.047
8	0	A	1	5%	0.15	91	1.053	44	0.25	A	1	5%	0.15	191	1.113
9	0	A	1	5%	0.25	187	1.079	45	0.25	A	1	5%	0.25	245	1.080
10	0	A	0	5%	0.08	59	1.052	46	0.25	A	0	5%	0.08	130	1.062
11	0	A	0	5%	0.15	208	1.091	47	0.25	A	0	5%	0.15	179	1.109
12	0	A	0	5%	0.25	272	1.098	48	0.25	A	0	5%	0.25	286	1.135
13	0	A	1	HSS	0.08	58	1.064	49	0.25	A	1	HSS	0.08	139	1.027
14	0	A	1	HSS	0.15	160	1.063	50	0.25	A	1	HSS	0.15	207	1.046
15	0	A	1	HSS	0.25	254	1.045	51	0.25	A	1	HSS	0.25	245	1.059
16	0	A	0	HSS	0.08	202	1.070	52	0.25	A	0	HSS	0.08	144	1.045
17	0	A	0	HSS	0.15	178	1.051	53	0.25	A	0	HSS	0.15	180	1.067
18	0	A	0	HSS	0.25	199	1.065	54	0.25	A	0	HSS	0.25	228	1.107
19	0	S*	1	8%	0.08	105	1.035	55	0.25	S	1	8%	0.08	193	1.059
20	0	S	1	8%	0.15	112	1.054	56	0.25	S	1	8%	0.15	196	1.060
21	0	S	1	8%	0.25	169	1.017	57	0.25	S	1	8%	0.25	183	1.044
22	0	S	0	8%	0.08	132	1.017	58	0.25	S	0	8%	0.08	112	1.087
23	0	S	0	8%	0.15	154	1.050	59	0.25	S	0	8%	0.15	208	1.060
24	0	S	0	8%	0.25	205	1.034	60	0.25	S	0	8%	0.25	170	1.067
25	0	S	1	5%	0.08	143	1.071	61	0.25	S	1	5%	0.08	75	1.077
26	0	S	1	5%	0.15	161	1.036	62	0.25	S	1	5%	0.15	185	1.079
27	0	S	1	5%	0.25	174	1.032	63	0.25	S	1	5%	0.25	217	1.160
28	0	S	0	5%	0.08	150	1.031	64	0.25	S	0	5%	0.08	145	1.067
29	0	S	0	5%	0.15	154	1.080	65	0.25	S	0	5%	0.15	158	1.074
30	0	S	0	5%	0.25	164	1.069	66	0.25	S	0	5%	0.25	158	1.084
31	0	S	1	HSS	0.08	129	1.048	67	0.25	S	1	HSS	0.08	139	1.075
32	0	S	1	HSS	0.15	114	1.058	68	0.25	S	1	HSS	0.15	161	1.062
33	0	S	1	HSS	0.25	148	1.066	69	0.25	S	1	HSS	0.25	172	1.078
34	0	S	0	HSS	0.08	121	1.048	70	0.25	S	0	HSS	0.08	126	1.044
35	0	S	0	HSS	0.15	105	1.041	71	0.25	S	0	HSS	0.15	144	1.065
36	0	S	0	HSS	0.25	137	1.045	72	0.25	S	0	HSS	0.25	153	1.047

A: Asymmetric; S: Symmetric

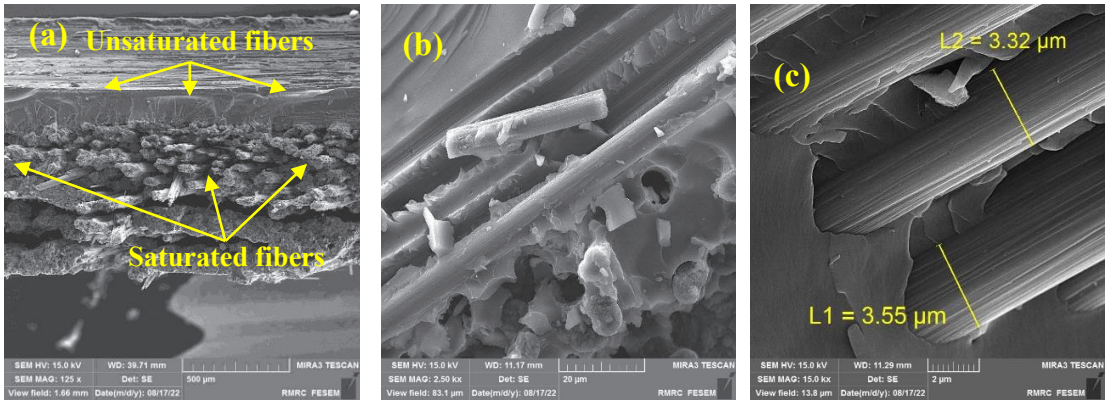

Fig. 3. SEM images of CFRP laminates.

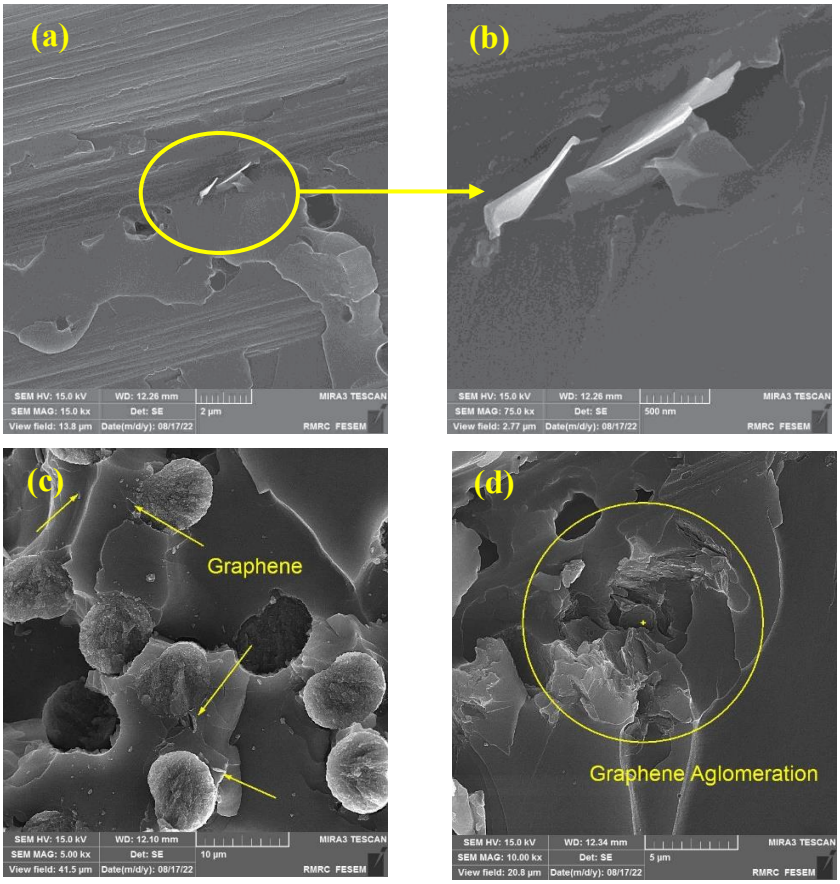

Fig. 4. SEM images of CFRP/GNP laminates

at the bottom are saturated effectively. Fig. 3(b) shows carbon fibers and the epoxy resin in which the carbon fibers are pre-impregnated in the epoxy matrix. That is shown epoxy adhesives are attached to the carbon fibers and strengthen the attached section. Fig. 3(c) shows unidirectional carbon fibers with a diameter of approximately 3.3 mm. The fibers were aligned in one direction and saturated by the hand layup method.

Fig. 4 demonstrates the CFRP/GNP composites. In Fig. 4(a), the epoxy resin with GNPs is demonstrated. Moreover, in Fig. 4(b), to show the GNPs in the composite, a high-magnitude SEM image was taken from Fig. 4(a) that shows one GNP. That indicates the GNP size is about 500 nm. Besides, Fig. 4(c) shows GNPs distribution in carbon fiber/epoxy matrix. That indicates GNPs distribution is well

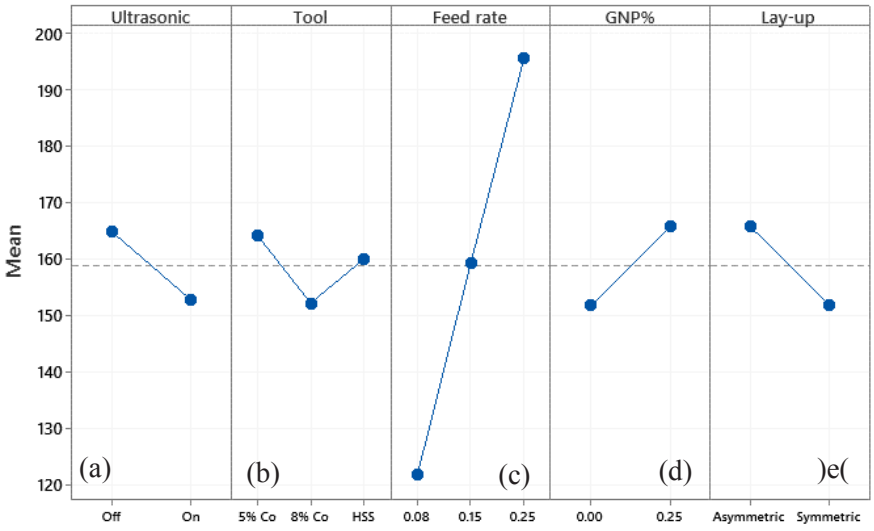

Fig. 5. Main effects plot for thrust force.

Table 4. ANOVA results for thrust force

Source	DF	SS	MS	Contribution %	F	P
Lay-up	1	3431	3430.7	1.87	2.05	0.157
Ultrasonic	1	2628	2628.1	1.43	1.57	0.214
GNP%	1	3598	3598.3	1.96	2.15	0.147
Feed rate	2	65127	32563.4	35.48	19.48	0.000
Tool	2	1782	890.9	0.97	0.53	0.589
Error	64	106983	1671.6	58.29		
Total	71	183548		100		

which induces suitable mechanical influence. However, in some places, GNPs are agglomerated and cause specimen brittleness is shown in Fig. 4(d). In these agglomerated structures, the epoxy and GNP interfacial load transfer has weakened [35], and therefore by imposing mechanical force such as drilling force, the breakage has occurred more easily.

3- 2- Thrust force

Examining thrust force is of great importance to improve tool life and machining performance which is required for planning the machining process of CFRP workpieces [36]. The influence of machining and materialistic parameters on thrust force is illustrated in Fig. 5 as a main effects plot.

ANOVA was also conducted to identify which factor is more influential on the process quality characteristics. ANOVA results for thrust force have been presented in Table 4. As declared by researchers, P-value < 0.05 shows that the parameter is significant [37]. It is inferred from Table 6 that the P-value for the feed rate is lower than 0.05 implying the feed rate factor has the most influence on the thrust force. Besides, each parameter's effects on thrust force are shown in the pie chart (Fig. 6).

In Fig. 5(a) ultrasonic vibration reduces thrust force compared to CD. This is due to interrupted impacts on the CFRP sample which causes fiber breakage more easily [38]. Besides, the produced chips evacuate from the drilling zone easily. Moreover, the thrust force plot in UVAD is interrupted which induces a lower average thrust force compared to CD.

As shown in Fig. 5(b), the effect of tool type on thrust force is evident. HSS tools are widely used in the industry due to their cost-effectiveness and strength. However, the addition of cobalt to HSS tools enhances their wear resistance and durability. The HSS-Co drills, which contain 5-8% cobalt, demonstrate a significant reduction in thrust force, with HSS-8% cobalt exhibiting the lowest thrust force. The inclusion of cobalt allows for higher feed rates when drilling CFRPs, as it improves the tool's heat resistance and overall robustness.

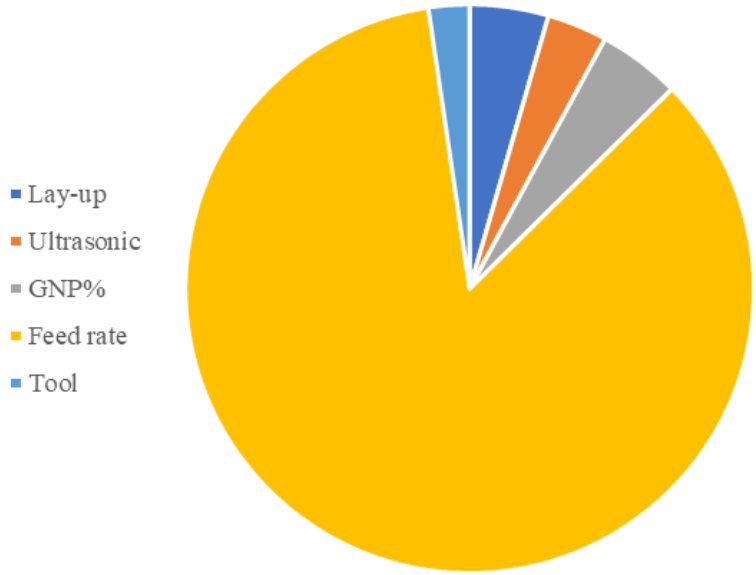

Fig. 6. Contribution% for thrust force.

As can be seen from Fig. 5(c), the thrust force amount increases dramatically as the feed rate is elevated. This is principally because the elevated feed rate causes an increase in cutting depth per revolution and the drilling tool cuts off larger material volumes per revolution [39]. Therefore, the thrust force gets larger. In addition, in case of larger feed rates, the tool pushes down the CFRP instead of cutting carbon fibers which produces a larger thrust force.

Based on Fig. 5(d), that indicates GNP adding to CFRP leads to thrust force increment that is due to higher CFRP/GNP strength compared to CFRP. Çelik et al. [40] stated that GNP addition increases the tensile strength of the CFRP. Besides, GNP has a good compatibility with carbon fibers and results in higher strength which makes the composite sample difficult to machine. This compatibility was previously shown in SEM images (Fig. 4).

Fig. 5(e) shows the effect of lay-up arrangement on thrust force. That shows a symmetrical arrangement causes lower thrust force compared to an asymmetrical one. That could be due to the thermal expansion coefficient difference between CFRP layers which is lower in symmetrical ones. For this reason, the asymmetrical samples after the curing and cooling stage will be formed as a curved shape. Hence for drilling these curved-shape CFRPs, another force is also required to overcome the bending resistance of the sample.

3- 3- Delamination

The drilling-induced delamination generally occurs at the entry and exit part of the drilled hole. The maximum diameter that surrounds the drilled hole is called delamination. Various parameters' influence is demonstrated in Fig. 7.

ANOVA results for delamination are offered in Table 5. It is inferred from the results, that the P-value is less than 0.05 for GNP%, feed rate, and tool type implying these parameters are important and should be given more consideration. Besides, each parameter's effects on delamination are shown in the pie chart (Fig. 6).

UVAD process compared to CD enhances the drilled hole quality which is shown in Fig. 7(a). That is because of the interrupted nature of the UVAD process which helps in fiber cutting and reduces machining-induced damages [4, 41]. In the UVAD process, tool wear happens with delay [42, 43]. Increased tool life in UVAD makes it suitable for fiber-reinforced composites processing. According to Fig. 9, the produced hole in UVAD is cleaner compared to the created hole in CD. Besides, as is seen in Fig. 9, the fiber pull-out length is decreased in UVAD which is due to the interrupted impacts in UVAD process.

As shown in Fig. 7(b), drilling with the HSS-8%Co tool results in significantly lower delamination compared to the other tool types. The addition of cobalt enhances the tool's mechanical properties, such as its hardness and wear resistance, which is particularly beneficial when drilling composite materials like CFRPs. Increasing the cobalt content in HSS tools up to 8% improves the tool's ability to withstand the high forces and heat generated during drilling, resulting in reduced delamination around the drilled hole.

In contrast, the HSS-5%Co tool, which contains a lower percentage of cobalt, induces more delamination. This is because the lower cobalt content leads to a reduction in the tool's strength and resistance to wear, causing the tool to degrade more quickly under the abrasive conditions of CFRP

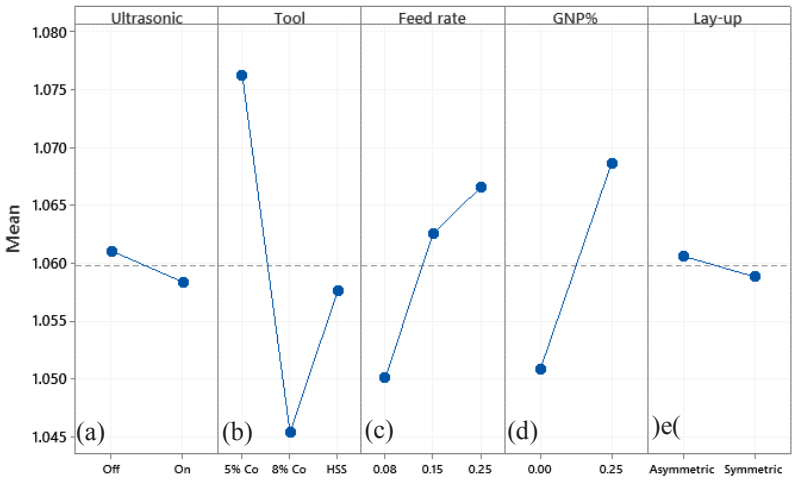

Fig. 7. Main effects plot for delamination.

Table 5. ANOVA results for delamination.

Source	DF	SS	MS	Contribution %	F	P
Lay-up	1	0.000057	0.000057	0.12	0.14	0.707
Ultrasonic	1	0.000131	0.000131	0.28	0.33	0.569
GNP%	1	0.005745	0.005745	12.29	14.33	0.000
Feed rate	2	0.003544	0.001772	7.58	4.42	0.016
Tool	2	0.011611	0.005806	24.84	14.48	0.000
Error	64	0.025660	0.000401	54.89		
Total	71	0.046749		100.00		

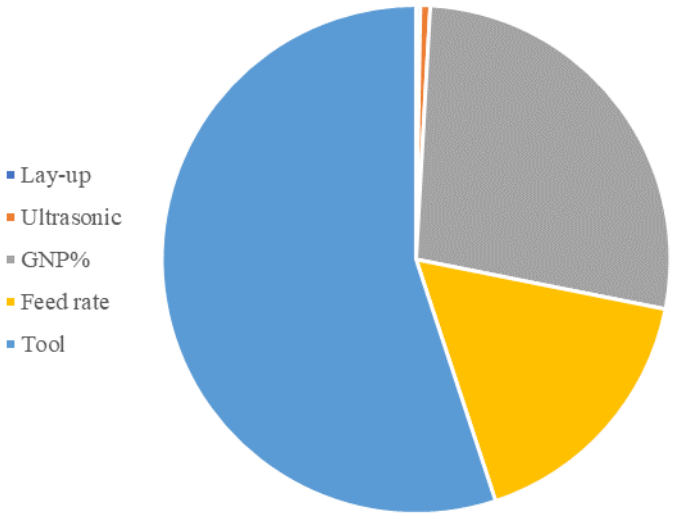

Fig. 8. Contribution% for delamination.

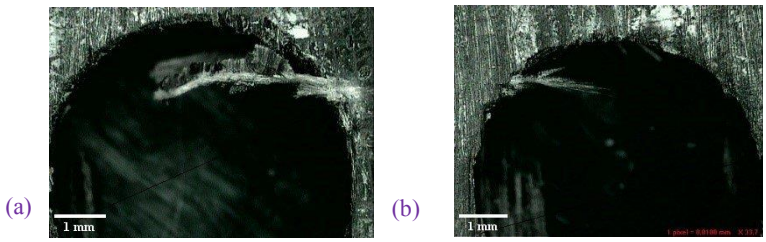

Fig. 9. Illustration of the drilled holes that are processed by a) CD, b) UVAD.

Fig. 10. Illustration of the drilled holes by a) HSS, b) HSS-5% Co, c) HSS-8% Co.

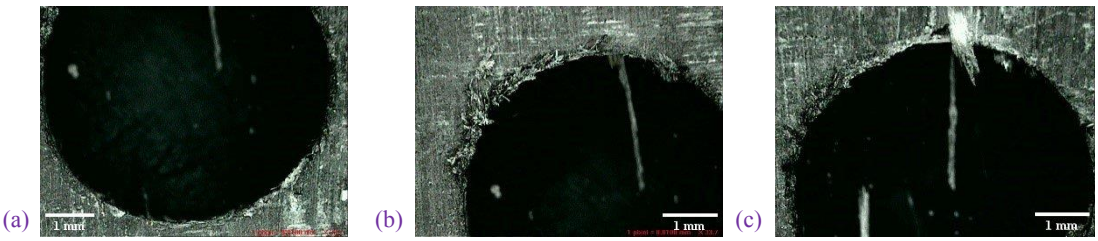

Fig. 11. Illustration of the drilled holes in the feed rate of a) 0.08, b) 0.15, c) 0.25 mm/rev.

drilling. As a result, the interaction between the tool and the material is less controlled, leading to larger delamination damage.

Interestingly, while the standard HSS tool without cobalt performs better than the HSS-5%Co tool in terms of delamination, it still does not match the performance of the HSS-8%Co tool. The HSS-8%Co tool provides the optimal balance between strength, wear resistance, and heat management, resulting in the least delamination and the best performance for drilling CFRPs. This is confirmed by the data in Fig. 10, which shows that the HSS-8%Co tool consistently outperforms the other tools in minimizing delamination damage.

Moreover, the feed rate parameter has the most influence on delamination value based on previous researches [44]. As shown in Fig. 7(c), at lower feed rates, the carbon fibers are cut easily which causes lower delamination. However, in higher feed rates, the fibers are pulled and afterward cut which induces low hole quality and larger delamination (Fig. 11). In addition, higher feed rates produce larger thrust forces based on Fig. 5 that destroys around the hole. According to Fig. 11, which is obtained in higher feed rate values, the fibers are pulled and remain uncut after drilling.

As depicted in Fig. 7(d), GNP addition causes a larger delamination value around the hole. That could be due to higher CFRP strength in case of GNP addition. That was also shown in Fig. 5, higher cutting force is produced in CFRP/GNP specimens compared to CFRP ones. Therefore, the fibers pulled while drilling and destroy the hole peripheral (Fig. 12)

As demonstrated in Fig. 7(e), there is an identical difference between the delamination result of asymmetric and symmetric lay-up arrangement. The results indicated delamination is reduced by symmetrical lay-up. That

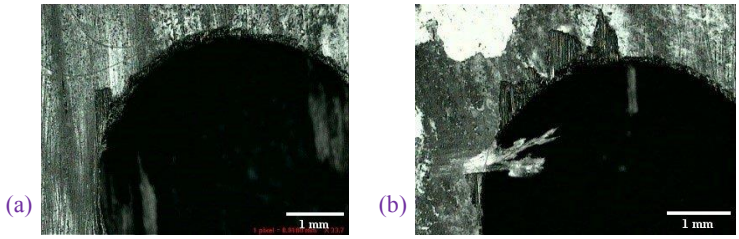

Fig. 12. Illustration of the drilled holes in a) CFRP, b) CFRP/GNP.

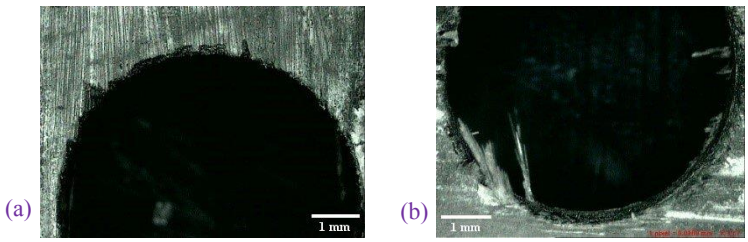

Fig. 13. Illustration of the drilled holes in CFRP with a) Symmetrical, b) Asymmetrical lay-up.

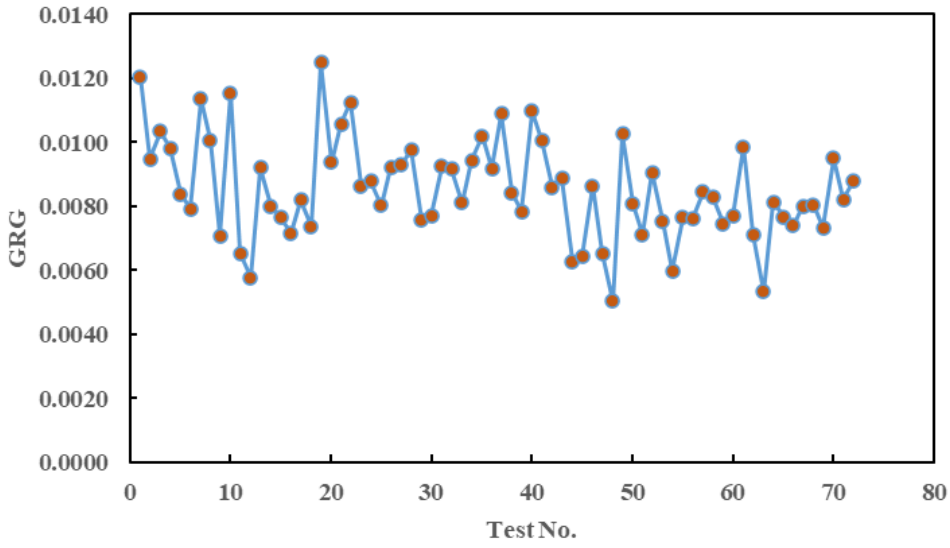

Fig. 14. GRA values obtained from 72 data.

was stated by other researchers that ply orientation has an influential effect on mechanical cracks and damages [45]. The reason of this fact can be due to the lower thermal expansion coefficient between layers in symmetrical lay-up comparing to asymmetrical ones. Hence, the residual stress that is created during the curing and cooling step, will be decreased in symmetrical plies. Since delamination is a side effect of residual stress [46-48], the delamination in symmetrical lay-up specimens is reduced. Besides, as noted previously, the asymmetric specimens are in curved shapes and are capable of delaminating due to bending characteristics. The symmetric specimens are flat and have no curvature which restricts delamination. Fig. 13 indicates the difference between the produced holes in symmetrical and asymmetrical lay-up.

4- Optimization using GRA

The normalized values and related GRC and GRG values and ranks for thrust force and F_d factors are presented in Table 6.

Besides, Fig. 14 demonstrates the overall GRG values. It is seen that the maximum GRG value occurs in test number of 19 which causes the lowest thrust force and F_d value. This

Table 6. Values of Grey relational analysis

No.	Normalized values		GRC		GRG value	No.	Normalized values		GRC		GRG value
	Force	F_d	Force	F_d			Force	F_d	Force	F_d	
1	0.0820	0.0713	0.8592	0.8751	0.0120	37	0.1680	0.1099	0.7485	0.8198	0.0109
2	0.4467	0.0982	0.5281	0.8358	0.0095	38	0.2746	0.3789	0.6455	0.5689	0.0084
3	0.1803	0.1626	0.7349	0.7546	0.0103	39	0.4508	0.3298	0.5259	0.6025	0.0078
4	0.3279	0.1170	0.6040	0.8104	0.0098	40	0.1598	0.1088	0.7578	0.8213	0.0110
5	0.4631	0.2269	0.5191	0.6879	0.0084	41	0.2295	0.1544	0.6854	0.7641	0.0101
6	1.0000	0.1193	0.3333	0.8074	0.0079	42	0.3975	0.2327	0.5571	0.6824	0.0086
7	0.0205	0.2398	0.9606	0.6759	0.0114	43	0.3689	0.2129	0.5755	0.7014	0.0089
8	0.1352	0.2550	0.7871	0.6623	0.0101	44	0.5451	0.6749	0.4784	0.4256	0.0063
9	0.5287	0.4363	0.4861	0.5340	0.0071	45	0.7664	0.4409	0.3948	0.5314	0.0064
10	0.0041	0.2468	0.9919	0.6695	0.0115	46	0.2951	0.3146	0.6289	0.6138	0.0086
11	0.6148	0.5158	0.4485	0.4922	0.0065	47	0.4959	0.6421	0.5021	0.4378	0.0065
12	0.8770	0.5673	0.3631	0.4685	0.0058	48	0.9344	0.8304	0.3486	0.3758	0.0050
13	0.1926	0.3275	0.7219	0.6042	0.0092	49	0.3320	0.0702	0.6010	0.8769	0.0103
14	0.4180	0.3216	0.5446	0.6085	0.0080	50	0.6107	0.2012	0.4502	0.7131	0.0081
15	0.8033	0.1977	0.3836	0.7167	0.0076	51	0.7664	0.2912	0.3948	0.6319	0.0071
16	0.5902	0.3743	0.4586	0.5719	0.0072	52	0.3525	0.1977	0.5865	0.7167	0.0091
17	0.4918	0.2398	0.5041	0.6759	0.0082	53	0.5000	0.3532	0.5000	0.5860	0.0075
18	0.5779	0.3368	0.4639	0.5975	0.0074	54	0.6967	0.6281	0.4178	0.4432	0.0060
19	0.0000	0.1263	1.0000	0.7983	0.0125	55	0.5533	0.2959	0.4747	0.6282	0.0077
20	0.2213	0.2620	0.6932	0.6562	0.0094	56	0.5656	0.2994	0.4692	0.6255	0.0076
21	0.4549	0.0000	0.5236	1.0000	0.0106	57	0.5123	0.1918	0.4939	0.7227	0.0084
22	0.3033	0.0012	0.6224	0.9977	0.0113	58	0.2213	0.4936	0.6932	0.5032	0.0083
23	0.3934	0.2292	0.5596	0.6856	0.0086	59	0.6148	0.3006	0.4485	0.6245	0.0075
24	0.6025	0.1158	0.4535	0.8120	0.0088	60	0.4590	0.3520	0.5214	0.5868	0.0077
25	0.3484	0.3801	0.5894	0.5681	0.0080	61	0.0697	0.4199	0.8777	0.5435	0.0099
26	0.4221	0.1357	0.5422	0.7866	0.0092	62	0.5205	0.4351	0.4900	0.5347	0.0071
27	0.4754	0.1064	0.5126	0.8245	0.0093	63	0.6516	1.0000	0.4342	0.3333	0.0053
28	0.3770	0.0959	0.5701	0.8391	0.0098	64	0.3566	0.3509	0.5837	0.5876	0.0081
29	0.3934	0.4421	0.5596	0.5307	0.0076	65	0.4098	0.4023	0.5495	0.5541	0.0077
30	0.4344	0.3673	0.5351	0.5765	0.0077	66	0.4098	0.4678	0.5495	0.5166	0.0074
31	0.2910	0.2152	0.6321	0.6991	0.0092	67	0.3320	0.4035	0.6010	0.5534	0.0080
32	0.2295	0.2865	0.6854	0.6357	0.0092	68	0.4221	0.3123	0.5422	0.6156	0.0080
33	0.3689	0.3439	0.5755	0.5925	0.0081	69	0.4672	0.4257	0.5169	0.5401	0.0073
34	0.2582	0.2152	0.6595	0.6991	0.0094	70	0.2787	0.1871	0.6421	0.7277	0.0095
35	0.1926	0.1696	0.7219	0.7467	0.0102	71	0.3525	0.3380	0.5865	0.5967	0.0082
36	0.3238	0.1977	0.6070	0.7167	0.0092	72	0.3893	0.2094	0.5622	0.7049	0.0088

test condition includes a symmetric sample with no GNP that was machined by 8% cobalt HSS tool, a feed rate of 0.08 mm/rev, and ultrasonic vibration assistance. On the other hand, because the optimal parameter combination is among the conducted experiments, no further experiment is required for the confirmation step.

5- Conclusions

This study analyzed the effects of mechanical and material parameters on thrust force and delamination during the drilling of CFRPs, using a full factorial design of experiments. Key findings include:

SEM analysis shows suitable nanoparticle distribution and carbon fibers/epoxy resin impregnation.

ANOVA results showed that feed rate was the most significant factor influencing thrust force and delamination, as shown by the ANOVA results ($p < 0.05$). Higher feed rates resulted in a dramatic increase in thrust force (e.g., from 78 N at 0.08 mm/rev to 302 N at 0.25 mm/rev), which caused severe fiber pull-out and hole quality degradation.

The inclusion of GNPs increased the composite's strength, resulting in higher thrust forces and larger delamination values. As a result, a larger force is applied to the composite causing the delamination value to increase.

The HSS-8% Co tool showed superior performance, reducing thrust force and delamination. For instance, at a feed rate of 0.08 mm/rev, a thrust force for the HSS-8% Co tool was 63 N, compared to 78 N for the HSS tool.

Symmetrical lay-up reduced delamination and thrust force compared to asymmetrical lay-up. For example, symmetrical lay-ups resulted in an average thrust force reduction of ~30% compared to asymmetrical configurations under similar conditions.

Ultrasonic Vibration: UVAD significantly lowered thrust force and delamination compared to conventional drilling (CD). This kind of movement makes the fibers to be cut easily and a cleaner drilled hole is provided. UVAD reduced thrust force by approximately 15% and improved hole quality by minimizing fiber pull-out.

Multi-objective optimization using GRA identified the optimal settings as: HSS-8% Co tool, feed rate of 0.08 mm/rev, symmetrical lay-up, and no GNP. These settings minimized thrust force and delamination, with thrust force reaching as low as 58 N and delamination at 1.027.

The results underscore the importance of parameter selection and optimization in achieving high-quality drilling of CFRPs. These findings provide a robust framework for industrial applications, particularly in advanced composites machining using UVAD.

Acknowledgements

Iran National Science Foundation (INSF) is gratefully acknowledged for financial support of this work (Project No. 99000063)

References

[1] N. Kundachira Subramani, Opto-electrical characteristics of poly (vinyl alcohol)/cesium zincate nanodielectrics, The Journal of Physical Chemistry C, 119(35) (2015) 20244-20255.

[2] M. Baraheni, S. Amini, Comprehensive optimization of process parameters in rotary ultrasonic drilling of CFRP aimed at minimizing delamination, International Journal of Lightweight Materials and Manufacture, 2(4) (2019) 379-387.

[3] A.P. Mouritz, Introduction to aerospace materials, Elsevier, 2012.

[4] A. Tabatabaeian, M. Baraheni, S. Amini, A.R.J.J.o.C.M. Ghasemi, Environmental, mechanical and materialistic effects on delamination damage of glass fiber composites: Analysis and optimization, Journal of Composite Materials, 53(26-27) (2019) 3671-3680.

[5] D. Liu, Y. Tang, W. Cong, A review of mechanical drilling for composite laminates, Composite structures, 94(4) (2012) 1265-1279.

[6] T. Barik, K. Pal, Prediction of TiAlN-and TiN-coated carbide tool wear in drilling of bidirectional CFRP laminates using wavelet packets of thrust–torque signatures, Journal of the Brazilian Society of Mechanical Sciences and Engineering, 44(8) (2022) 364.

[7] K. Starost, J. Njuguna, A review on the effect of mechanical drilling on polymer nanocomposites, in: IOP Conference Series: Materials Science and Engineering, IOP Publishing, 2014, pp. 012031.

[8] C. Lü, C. Guan, Y. Liu, Y. Cheng, B. Yang, PbS/polymer nanocomposite optical materials with high refractive index, Chemistry of materials, 17(9) (2005) 2448-2454.

[9] M. Baraheni, A. Tabatabaeian, S. Amini, A.R.J.C.P.B.E. Ghasemi, Parametric analysis of delamination in GFRP composite profiles by performing rotary ultrasonic drilling approach: Experimental and statistical study, Composites Part B: Engineering, 172 (2019) 612-620.

[10] Q. Wang, L. Zhu, Polymer nanocomposites for electrical energy storage, Journal of Polymer Science Part B: Polymer Physics, 49(20) (2011) 1421-1429.

[11] Y. Di, S. Iannace, E.D. Maio, L. Nicolais, Poly (lactic acid)/organoclay nanocomposites: thermal, rheological properties and foam processing, Journal of Polymer Science Part B: Polymer Physics, 43(6) (2005) 689-698.

[12] R. Taherian, Experimental and analytical model for the electrical conductivity of polymer-based nanocomposites, Composites Science and Technology, 123 (2016) 17-31.

[13] A. Kumar, K. Sharma, A.R. Dixit, A review of the mechanical and thermal properties of graphene and its hybrid polymer nanocomposites for structural applications, Journal of materials science, 54(8) (2019) 5992-6026.

[14] K. Giasin, S. Ayvar-Soberanis, An Investigation of burrs, chip formation, hole size, circularity and delamination

during drilling operation of GLARE using ANOVA, Composite Structures, 159 (2017) 745-760.

[15] K. Giasin, S. Ayvar-Soberanis, A. Hodzic, An experimental study on drilling of unidirectional GLARE fibre metal laminates, Composite Structures, 133 (2015) 794-808.

[16] J. Sheikh-Ahmad, J. Davim, Tool wear in machining processes for composites, in: Machining technology for composite materials, Elsevier, 2012, pp. 116-153.

[17] S. Cao, H.N. Li, W. Huang, Q. Zhou, T. Lei, C. Wu, A delamination prediction model in ultrasonic vibration assisted drilling of CFRP composites, Journal of Materials Processing Technology, 302 (2022) 117480.

[18] S. Vigneshwaran, M. Uthayakumar, V. Arumugaprabu, Abrasive water jet machining of fiber-reinforced composite materials, Journal of Reinforced Plastics and Composites, 37(4) (2018) 230-237.

[19] B. Kavad, A. Pandey, M. Tadavi, H. Jakharia, A review paper on effects of drilling on glass fiber reinforced plastic, Procedia Technology, 14 (2014) 457-464.

[20] S. Arul, L. Vijayaraghavan, S. Malhotra, R. Krishnamurthy, The effect of vibratory drilling on hole quality in polymeric composites, International Journal of Machine Tools and Manufacture, 46(3-4) (2006) 252-259.

[21] N. Mohan, A. Ramachandra, S. Kulkarni, Influence of process parameters on cutting force and torque during drilling of glass–fiber polyester reinforced composites, Composite structures, 71(3-4) (2005) 407-413.

[22] V. Gaitonde, S. Karnik, J.C. Rubio, A.E. Correia, A. Abrao, J.P. Davim, A study aimed at minimizing delamination during drilling of CFRP composites, Journal of Composite Materials, 45(22) (2011) 2359-2368.

[23] Y. Zhang, X. Xu, Predicting the delamination factor in carbon fibre reinforced plastic composites during drilling through the Gaussian process regression, Journal of Composite Materials, 55(15) (2021) 2061-2068.

[24] T. Srinivasan, K. Palanikumar, K. Rajagopal, B. Latha, Optimization of delamination factor in drilling GFR–polypropylene composites, Materials and Manufacturing Processes, 32(2) (2017) 226-233.

[25] [25] N. Shetty, D. Shetty, G. Vijay, R. Shetty, Mechanical characterization and evaluation of delamination of polymer composite laminate, International Journal of Applied Engineering Research, 10(15) (2015) 35757-35769.

[26] H. Hocheng, C. Tsao, The path towards delamination-free drilling of composite materials, Journal of materials processing technology, 167(2-3) (2005) 251-264.

[27] R.K. Verma, K. Abhishek, S. Datta, S.S. Mahapatra, Fuzzy rule based optimization in machining of FRP composites, Turkish Journal of Fuzzy Systems, 2(2) (2011) 99-121.

[28] J.P. Davim, P. Reis, Study of delamination in drilling carbon fiber reinforced plastics (CFRP) using design experiments, Composite structures, 59(4) (2003) 481-487.

[29] V. Dhawan, K. Debnath, I. Singh, S. Singh, Prediction of forces during drilling of composite laminates using artificial neural network: a new approach, FME Transactions, 44(1) (2016) 36-42.

[30] P. Mayuet, A. Gallo, A. Portal, P. Arroyo, M. Alvarez, M. Marcos, Damaged area based study of the Break-IN and Break-OUT defects in the dry drilling of carbon fiber reinforced plastics (CFRP), Procedia Engineering, 63 (2013) 743-751.

[31] W. Cong, Z.J. Pei, Q. Feng, T.W. Deines, C. Treadwell, Rotary ultrasonic machining of CFRP: a comparison with twist drilling, Journal of Reinforced Plastics and Composites, 31(5) (2012) 313-321.

[32] W. Huang, S. Cao, H.N. Li, Q. Zhou, C. Wu, D. Zhu, K. Zhuang, Tool wear in ultrasonic vibration–assisted drilling of CFRP: a comparison with conventional drilling, The International Journal of Advanced Manufacturing Technology, 115(5-6) (2021) 1809-1820.

[33] N.D. Alexopoulos, Z. Paragkamian, P. Poulin, S.K. Kourkoulis, Fracture related mechanical properties of low and high graphene reinforcement of epoxy nanocomposites, Composites Science and Technology, 150 (2017) 194-204.

[34] W.-C.J.I.J.o.M.T. Chen, Manufacture, Some experimental investigations in the drilling of carbon fiber-reinforced plastic (CFRP) composite laminates, 37(8) (1997) 1097-1108.

[35] M. Li, H. Zhou, Y. Zhang, Y. Liao, H. Zhou, The effect of defects on the interfacial mechanical properties of graphene/epoxy composites, RSC advances, 7(73) (2017) 46101-46108.

[36] Y. Song, H. Cao, W. Zheng, D. Qu, L. Liu, C.J.C.S. Yan, Cutting force modeling of machining carbon fiber reinforced polymer (CFRP) composites: A review, 299 (2022) 116096.

[37] N. Feito, A. Muñoz-Sánchez, A. Díaz-Álvarez, M. Miguelez, Multi-objective optimization analysis of cutting parameters when drilling composite materials with special geometry drills, Composite Structures, 225 (2019) 111187.

[38] S. Amini, M. Baraheni, A.J. Mardiha, Parametric investigation of rotary ultrasonic drilling of carbon fiber reinforced plastics, Proceedings of the Institution of Mechanical Engineers, Part E: Journal of Process Mechanical Engineering, 232(5) (2018) 540-554.

[39] X. Qiu, P. Li, Q. Niu, A. Chen, P. Ouyang, C. Li, T.J. Ko, Influence of machining parameters and tool structure on cutting force and hole wall damage in drilling CFRP with stepped drills, The International Journal of Advanced Manufacturing Technology, 97 (2018) 857-865.

[40] Y.H. Çelik, E. Kilickap, N. Koçyiğit, Evaluation of

drilling performances of nanocomposites reinforced with graphene and graphene oxide, The International Journal of Advanced Manufacturing Technology, 100 (2019) 2371-2385.

[41] M. Baraheni, S. Amini, Feasibility study of delamination in rotary ultrasonic-assisted drilling of glass fiber reinforced plastics, Journal of Reinforced Plastics and Composites, 37(1) (2018) 3-12.

[42] E. Yarar, S. Karabay, Investigation of the effects of ultrasonic assisted drilling on tool wear and optimization of drilling parameters, CIRP Journal of Manufacturing Science and Technology, 31 (2020) 265-280.

[43] A. Sharma, V. Jain, D. Gupta, Characterization of chipping and tool wear during drilling of float glass using rotary ultrasonic machining, Measurement, 128 (2018) 254-263.

[44] E. Kilickap, Optimization of cutting parameters on delamination based on Taguchi method during drilling of GFRP composite, Expert systems with applications, 37(8) (2010) 6116-6122.

[45] S. Rouquie, M. Lafarie-Frenot, J. Cinquin, A. Colombaro, Thermal cycling of carbon/epoxy laminates in neutral and oxidative environments, Composites Science and Technology, 65(3-4) (2005) 403-409.

[46] R. Hussein, A. Sadek, M. Elbestawi, M. Attia, Elimination of delamination and burr formation using high-frequency vibration-assisted drilling of hybrid CFRP/Ti6Al4V stacked material, The International Journal of Advanced Manufacturing Technology, 105 (2019) 859-873.

[47] T. Wu, S. Degener, S. Tinkloh, A. Liehr, W. Zinn, J. Nobre, T. Tröster, T. Niendorf, Characterization of residual stresses in fiber metal laminate interfaces–A combined approach applying hole-drilling method and energy-dispersive X-ray diffraction, Composite Structures, 299 (2022) 116071.

[48] A. Tabatabaeian, A.R. Ghasemi, M.M. Shokrieh, B. Marzbanrad, M. Baraheni, M. Fotouhi, Residual stress in engineering materials: a review, Advanced Engineering Materials, 24(3) (2022) 2100786.

HOW TO CITE THIS ARTICLE

M. Baraheni, S. Amini, Ultrasonic Vibratory Drilling Carbon Fiber/Graphene Nanoparticle Reinforced Polymers to Produce Desired Hole Quality: Experimental Analysis and Optimization, AUT J. Mech Eng., 9(2) (2025) 195-210.

DOI: 10.22060/ajme.2025.23532.6143